Journal of Thermal Analysis, Vol. 53 (1998) 533-545

Dedicated to Professor Ferenc Paulik on the occasion of his 75th birthday

SOL–GEL PROCESSING OF COPPER-CHROMIUM CATALYSTS FOR ESTER HYDROGENATION

A. Kaddouri[1], *C. Mazzocchia*[1], *E. Tempesti*[2], *R. Nomen*[3] *and J. Sempere*[3]

[1]Department of Industrial Chemistry and Chemical Engineering, Politecnico di Milano
P.zza L. da Vinci 32 Milano, 20133 Italy
[2]Department Mater. Sci. Università degli studi di Brescia, via Valoti 9 Brescia 25123 Italy
[3]Institut Quimic de Sarrià, 0817 Barcelona, Spain

Abstract

Copper chromite catalysts were prepared by using a new metal organic precursor, $M(OR)_n$, which was dissolved in organic solvent, hydrolysed and condensed to form inorganic polymers containing M–O–M linkages. In the cases of Ba and Mn promotion, the corresponding metal oxide was admixed to the copper-chromium solution prior to gelification. After drying in helium atmosphere, the precursor was subjected to thermal treatment at different temperatures (373–873 K) and in different atmospheres (air, nitrogen or hydrogen). Both the catalysts and the industrial Engelhard catalyst were characterized by various techniques (TG–DTA, HTXRD, IR, BET, metallic copper surface area and porosimetry measurements) and evaluated for ester hydrogenation.

Keywords: Cu–Cr–O system, ester hydrogenation, sol–gel preparation

Introduction

Following the initial report by Adkins *et al.* in 1931 [1], copper chromite catalysts have been widely used in the production of higher alcohols from fatty acid esters by high-pressure hydrogen reduction. The most common way to prepare this catalyst is via the precipitation of the basic copper aluminium chromate [2]. With the use of oxalic acid, a new precursor [3] for the preparation of copper chromite catalyst has recently been reported. The resulting catalyst does not need to be reduced, whereas reduction is necessary for the traditional Adkins catalyst. In any case, it has been proved by several techniques that reduced copper is the active species in the hydrogenation reactions.

The present work reports the preparation of a new precursor of (undoped and doped) copper chromite catalyst: (MnO or BaO)/$Cu{\cdot}CuCr_2O_4$.

1418–2874/98/ $ 5.00

Akadémiai Kiadó, Budapest
Kluwer Academic Publishers, Dordrecht

Experimental

Sol–gel preparation

The catalyst was prepared (Fig. 1) by dissolving separately at 85°C, pure chromium oxide CrO_3, basic copper carbonate $CuCO_3{\cdot}Cu(OH)_2$ and barium oxide BaO or manganese acetate $Mn(CH_3COO)_2$ in liquid propionic acid under constant stirring. The dissolution of the Cu and Cr compounds was very slow. After some hours, the solutions became transparent. Particularly for the chromium solution the exact time of dissolution of the chromium oxide had to be carefully taken into account in order to avoid the precipitation of Cr(III) oxide (by reduction of the Cr(VI), which could take place after a long period under acidic conditions. The above solutions were subsequently mixed, hydrolysed with a few drops of distilled water and evaporated; the resulting gel (a polymer built up from M–O–M or M–(μOH)–M bonds) was frozen with liquid nitrogen, which led to a powder form of the gel as a solid-state Cu, Cr and Mn or Ba propionate precursor.

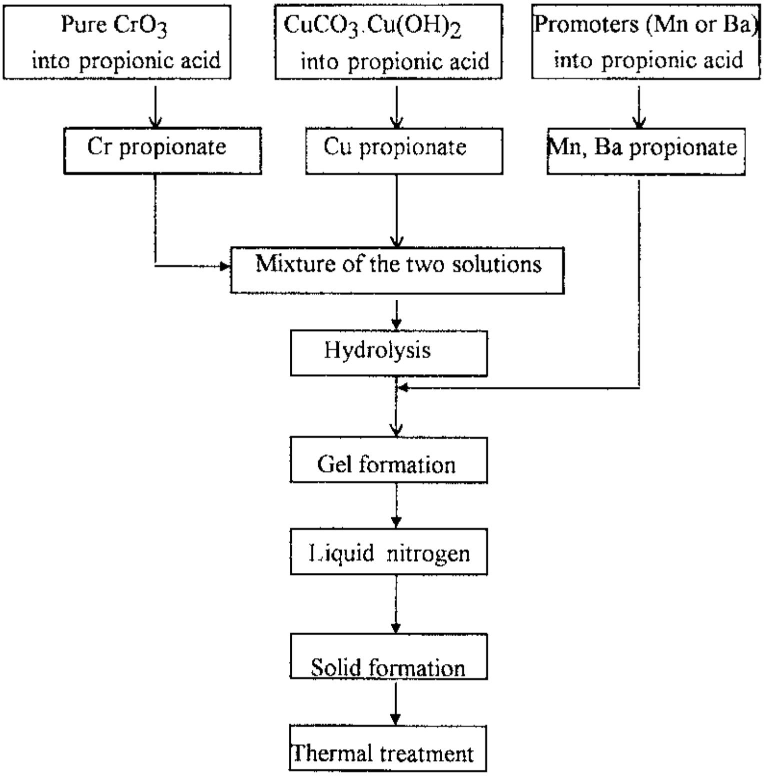

Fig. 1 Summary of copper chromite catalyst preparation by sol–gel method

Characterization

The evolution of the decomposition of the precursors was studied under air and under nitrogen, using a Seiko Instruments thermogravimetric analyser (TG–DTA–DTG). The samples, weighing approximately 20 mg, were placed in quartz crucibles and heated up to 500°C (1–10°C min^{-1}). The gas feed (air or nitrogen) was 6 l h^{-1}.

Porosimetry and BET surface measurements were performed on a Quantasorb (Quantachrome Co.) instrument, while the metallic copper surface areas were determined from the dissociative adsorption of nitrous oxide [4].

H.T. X-ray diffraction patterns of the samples were recorded on a Siemens D 5000 diffractometer with filtered CuK_α radiation (count time of 1 s in the range $2\Theta=10–70°$). The samples were also characterized by FT-IR (Perkin Elmer Mod. 1760, KBr pellets).

Catalyst evaluation

Ester hydrogenation tests were performed with 15 g of catalyst and 250 ml of an ester in a batch (500 ml volume) stainless steel cylindrical reactor (EZE-SEAL). The hydrogen pressure and working temperature were 190–220 atm and 230–270°C, respectively, with a stirring velocity of 2000 rpm.

The reaction product was separated and analysed on a Porapak QS column linked to a flame ionization detector.

Results and discussion

Thermal activation of the precursor

The behaviour of CuCrPP during thermal activation, and consequently the phase composition of the final catalyst, can be better understood if the decomposition patterns of the simple copper and chromium propionates are taken into account. The preparation method employed was the same as reported in the Experimental section.

Cu propionate precursor (CuPP)

The decomposition of Cu propionate in air (Fig. 2a) furnished an endothermic peak between ambient temperature and 100°C, with a mass loss of about 6.5% (H_2O), followed by three exothermic peaks between 200 and 230°C, which can be attributed to the decomposition of propionate groups and the crystallization of CuO. The heat produced during these three exothermic phenomena was 0.85, 1.25 and –1.864 kJ g^{-1}, respectively. The total mass loss for the decomposition of CuPP was estimated as 68.8%.

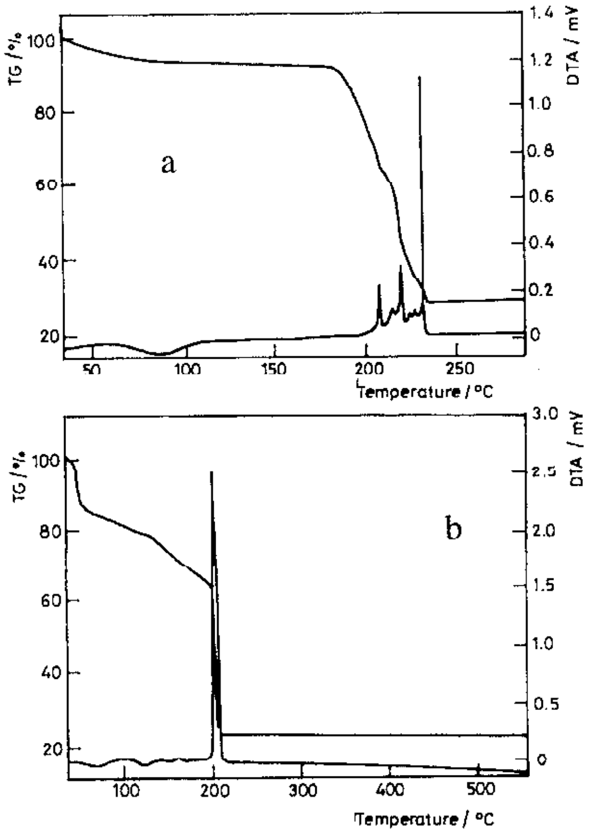

Fig. 2 Decomposition under air of sol–gel precursor a) CuPP, b) CrPP

Cr propionate precursor (CrPP)

In air, the decomposition of CrPP (Fig. 2b) yielded an endothermic peak accompanied by a mass loss of 23.5% (H_2O), followed by a second mass loss of about 9.7%, relating to the loss of free propionic acid, and a sharp exothermic peak at 200°C (mass loss of 42.8%), due to the simultaneous decomposition of propionate groups and the crystallization of chromium oxide. The heat of precursor decomposition at 200°C was estimated to be -12.9 kJ g^{-1}. The total mass loss during CrPP decomposition was found to be 76%.

The overall processes of decomposition of CuPP and CrPP can be characterized by the following equations:

$$Cu(C_3H_5O_2)_2 + 7O_2 \rightarrow CuO + 6CO_2 + 5H_2O$$

$$Cr_2(C_3H_5O_2)_3 + 11.25O_2 \rightarrow Cr_2O_3 + 9CO_2 + 7.5H_2O$$

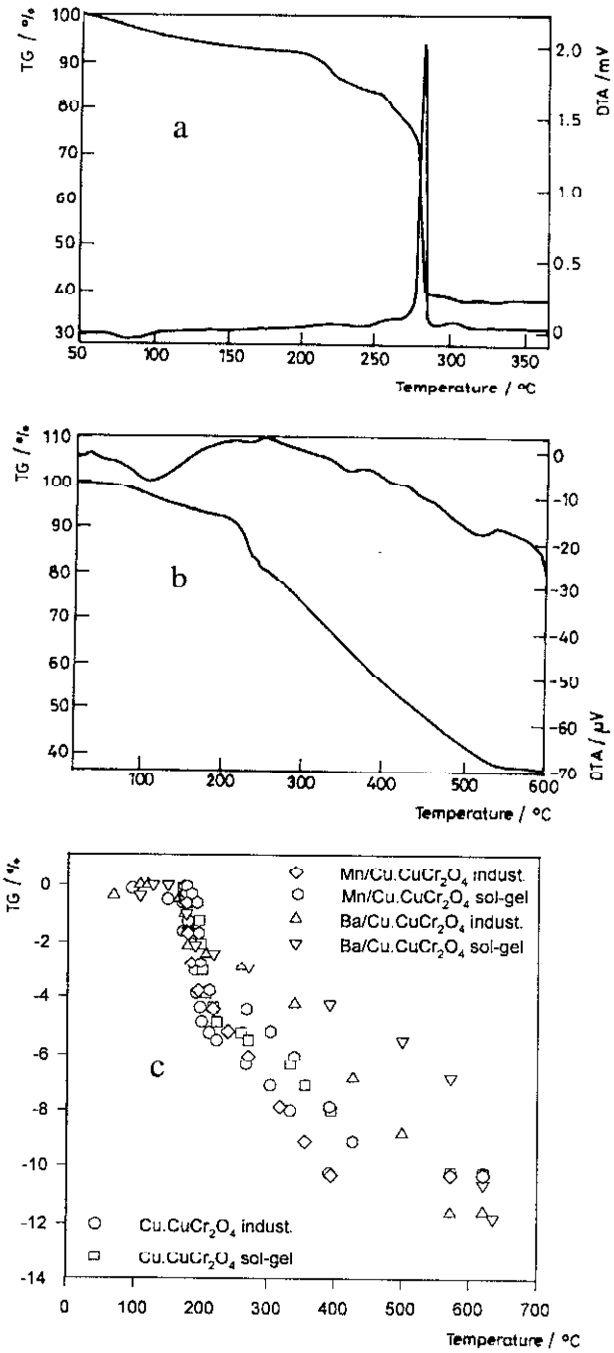

Fig. 3 Decomposition of CuCrPP sol–gel precursor a) under air, b) under N_2, c) TG in hydrogen atmosphere of industrial and sol–gel copper chromite catalysts

In air, the mass loss between 170 and 250°C during the decomposition of the Cu and Cr precursors was 62.3% (62.06% theor.) and 52.5%) 52.9% theor.), respectively, in agreement with the above equations.

CuCr propionate precursor (CuCrPP)

The powder obtained was treated under different atmospheres (air, nitrogen or hydrogen) at various temperatures in the range 100–600°C, to yield copper chromite and copper oxide phases. The copper chromite activation step is more important as it directly determines the catalytic performance of the catalyst. In order to elucidate the roles of the atmosphere and the heating rate on the precursor decomposition, several runs were performed at different heating rates under air, nitrogen or hydrogen. TG–DTA analyses of the sol–gel precursor demonstrated that heating at 10°C $\min^{-1}$ in the presence of air afforded a strong exothermic effect ($\Delta H > 21.3$ kJ g^{-1}) at nearly 280°C, corresponding to two distinct phenomena taking place simultaneously: propionate oxidation and copper(II) oxide crystallization. For a better evaluation of all the thermal effects and to avoid excessive heat flow and even explosive reactions at around 200–320°C, the heating rate was reduced (1°C $\min^{-1}$). Under these conditions (Fig. 3a), the existence of a first large endothermic peak between ambient temperature and 170°C was observed, and this was attributed to the loss of water and free propionic acid. The onset of the exothermic effect occurred at around 225°C. It was separately shown by HTXRD that the crystallization of copper chromite began after the precursor had been kept for 3 h at 250°C in air, and that it was necessary to heat up to 550°C to complete this (Fig. 4).

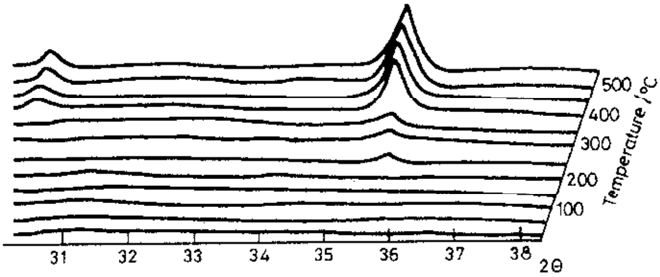

Fig. 4 HTXRD spectra of Mn/Cu·$CuCr_2O_4$ sol–gel catalyst

The thermogravimetric analyses performed in air (Fig. 3a) indicated that the mass loss amounted to 6.5% between 50 and 100°C (removal of water). Between 170 and 260°C, an abrupt increase in mass loss (15.2%) was observed; specifically, at around 230°C the mass loss was 7.5% which may be due to CH_3CH_2O or $CH_3CH_2CO_2$ radicals [5]. The final mass loss between 260 and 320°C was the most important (about 40.8%), and was due to the oxidation of the organic groups (propionate ligands). The total mass loss during the decomposition of the sol–gel precursor is estimated to be 62.5%.

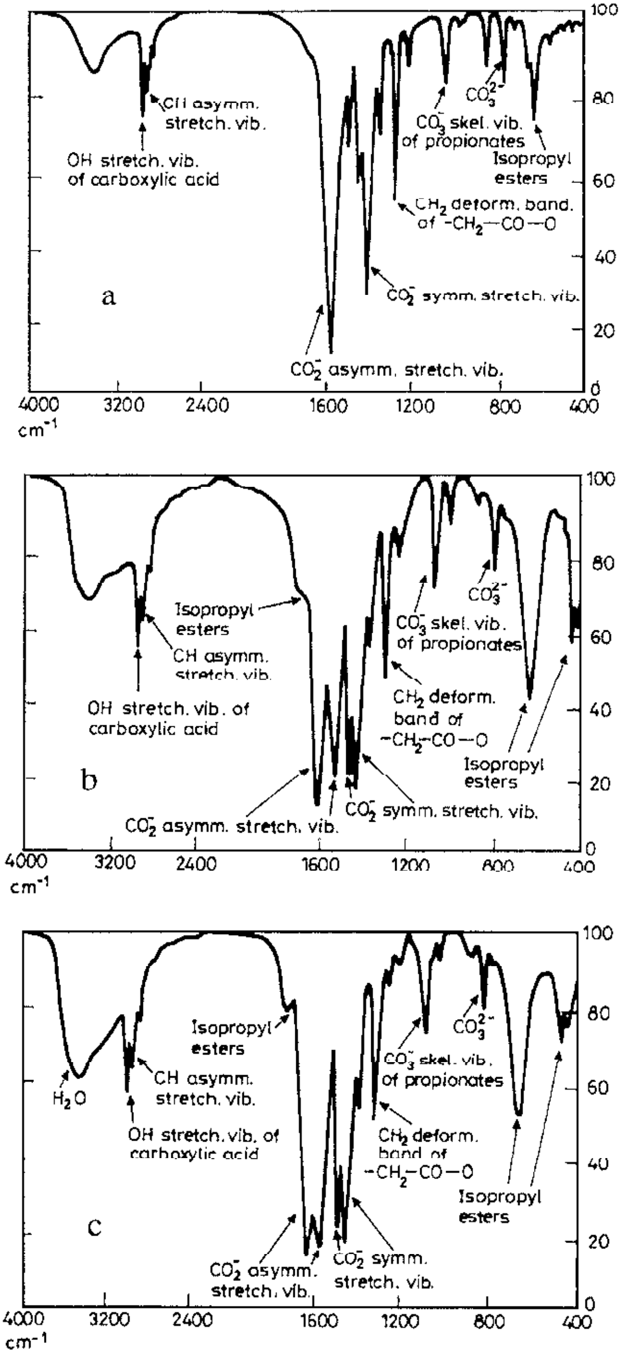

Fig. 5 FTIR spectra of sol–gel precursor a) CuPP, b) CrPP, c) CuCrPP

A similar study under nitrogen (Fig. 3b) revealed the same endothermic effect relating to the loss of water in the range between ambient and 170°C at a heating rate of 1°C min^{-1}, followed by a less pronounced exothermic effect. The following mass losses were observed: 6.3% between ambient temperature and 170°C (H_2O and free propionic acid), 13.1% between 170 and 250°C (≈7.05% at around 230°C, attributed to CH_3CH_2O or $CH_3CH_2CO_2$ radicals) and 43% between 250 and 550°C (propionate group decomposition with simultaneous crystallization). The total mass loss during the decomposition of the sol–gel precursor is estimated to be 62.4%.

It may be noted that under air the rate of decomposition of the precursor measured by TG analysis is sharper with respect to that under nitrogen (Fig. 3a *vs.* Fig. 3b). When the IR spectra of CuPP and CrPP are compared with those of CuCrPP (Fig. 5a, b, c), it can be seen that of CrPP (Fig. 5b) is quite similar to that of CuCrPP (Fig. 5c); in contrast, that of CuPP is completely different.

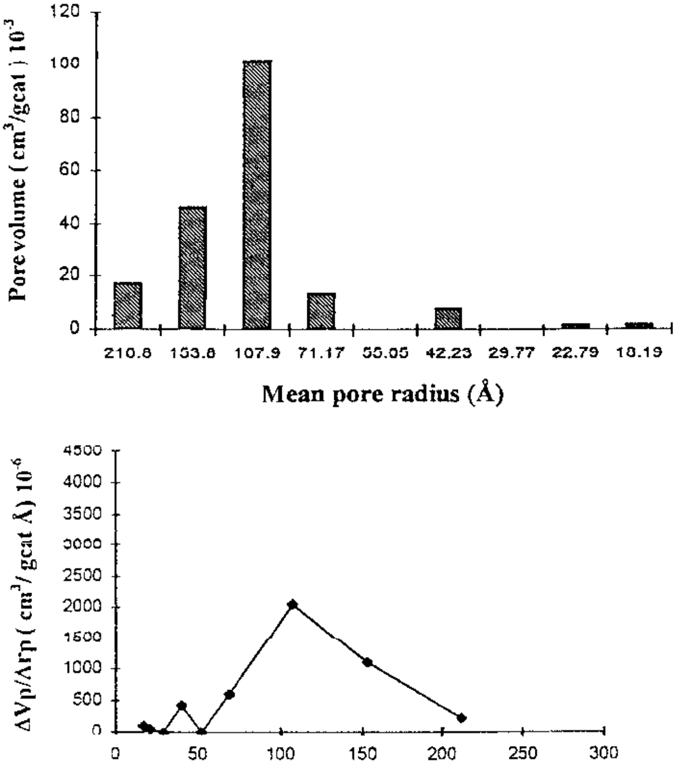

Fig. 6 Pore volume and pore size distribution of $Mn/Cu{\cdot}CuCr_2O_4$ industrial catalyst

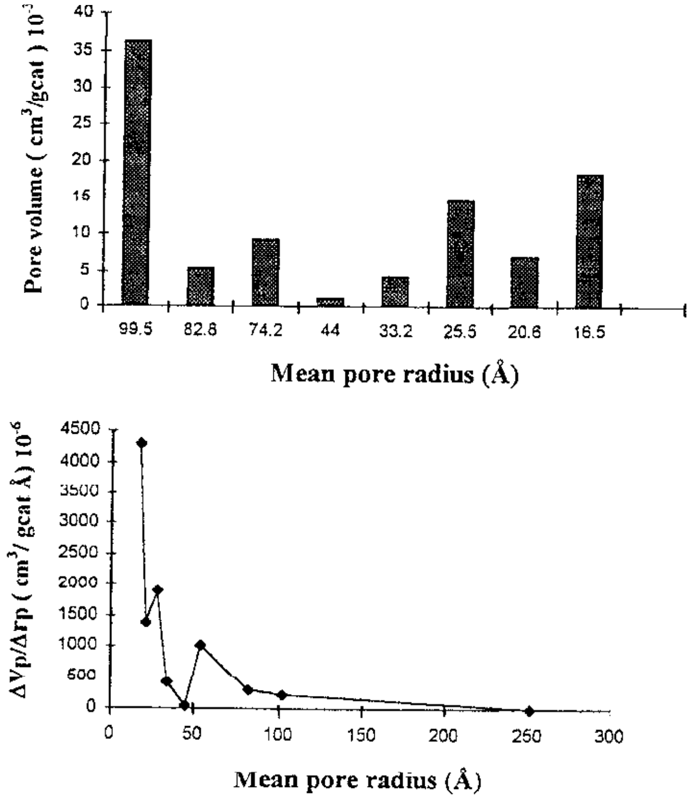

Fig. 7 Pore volume and pore size distribution of Mn/Cu·$CuCr_2O_4$ sol–gel catalyst

All these observations (thermal analyses and IR spectra) allow the conclusion that CuCrPP is not a mixture of the Cu and Cr-based propionate precursors even if the heat of decomposition for CuCrPP (–21.3 kJ g^{-1}) is almost equal to the sum (–20.8 kJ g^{-1}) of those for CrPP (–12.9 kJ g^{-1}) and CuPP (–3.96 kJ g^{-1}×2). The overall decomposition process for CuCrPP can be exemplified by the following equations:

in air:

$$2Cu(C_3H_5O_2)_2CrO_4+11.5O_2 \rightarrow CuO{\cdot}CuCr_2O_4+12CO_2+10H_2O$$

in nitrogen:

$$2Cu(C_3H_5O_2)_2CrO_4 \rightarrow Cu{\cdot}CuCr_2O_4+12CO+10H_2$$

This scheme is in agreement with the experimental results; the decomposition between 170 and 550°C amounts to 56.2% (52.4% theor.) in air, and to 55.8% (54.8% theor.) in nitrogen.

Porosimetry

The pore volume distribution and the form of the hysteresis loop were recorded for all the catalytic systems (Cu·$CuCr_2O_4$, Ba/Cu·$CuCr_2O_4$, and Mn/Cu·$CuCr_2O_4$), either commercially available or synthesized by the sol–gel procedure. The doped sol–gel-prepared copper chromite catalyst exhibited a predominantly microporous pore volume distribution, with a total pore volume and a total pore surface area respectively smaller or higher than those of the corresponding industrial product. As an example, Figs 6 and 7 depict the pore volume and pore size distribution *vs.* the mean pore radius for the commerical and the sol–gel Mn-doped copper chromite catalyst.

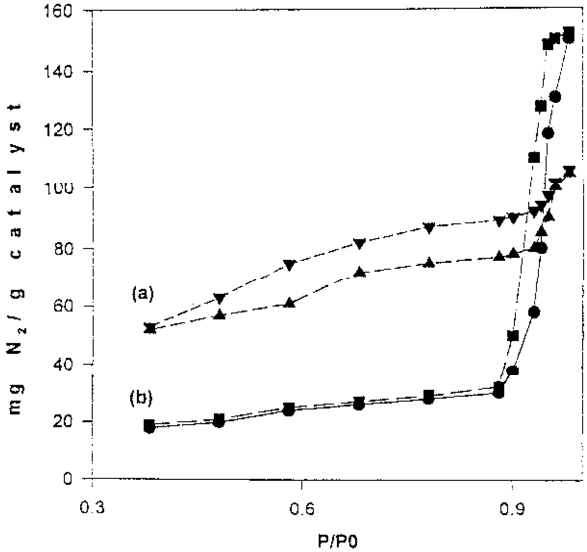

Fig. 8 Types of hysteresis loop of Mn-doped copper chromite a) sol–gel, b) industrial

The adsorption and desorption isotherms of nitrogen at 77 K for the sol–gel (a) and commercial (b) Mn-doped catalysts are reported in Fig. 8. The hysteresis loop obtained for the sol–gel catalyst spreads over a P/P_0 range from about 0.4 to 0.98, with a horizontal form, while the corresponding one for the commercial catalyst has a vertical form. On the other hand, the loop formed by the adsorption and desorption curves is less pronounced in the case of the commercial catalyst with respect to the sol–gel catalyst. This difference may be due to the presence of a large pore volume and a small surface area in the former catalyst and to a more complicated pore structure [6, 7] in the latter. Table 1 reports the data obtained on all the studied catalysts.

Table 1 Porosimetric parameters of the catalysts

Catalysts	Pore volume/ $cm^3\ g^{-1}$	Sum of pore area/ $m^2\ g^{-1}$	Mean radius/ Å
$Cu{\cdot}CuCr_2O_4$	0.123	29.2	84.7
$Cu{\cdot}CuCr_2O_4$ sol–gel	0.076	112	24.7
$Ba/Cu{\cdot}CuCr_2O_4$	0.186	60.4	61.6
$Ba/Cu{\cdot}CuCr_2O_4$ sol–gel	0.092	120	29.6
$Mn/Cu{\cdot}CuCr_2O_4$	0.187	34.1	109
$Mn/Cu{\cdot}CuCr_2O_4$ sol–gel	0.096	127	15.0

Catalytic tests

The catalytic activity was measured by making use of the equation $K=\ln[C_o/C_\tau]/\tau$, where C_o is the initial concentration of the ester and C_τ is the concentration at time τ.

Table 2 Hydrogenation of hexyl acetate and pentyl acetate on industrial and sol–gel prepared copper chromite-based catalysts

Catalysts	Reagent	Width of principal peak (30<2θ<45) at half-height	Yield/%	
			after 2 h	after 4 h
$Cu{\cdot}CuCr_2O_4$	hexyl acetate	0.28	60	86
$Cu{\cdot}CuCr_2O_4$ (sol–gel)	hexyl acetate	0.38	36	65*
$Ba/Cu{\cdot}CuCr_2O_4$	hexyl acetate	0.44	70	95
$Ba/Cu{\cdot}CuCr_2O_4$ (sol–gel)	hexyl acetate	0.50	42	72*
$Mn/Cu{\cdot}CuCr_2O_4$	hexyl acetate	0.48	86	99
$Mn/Cu{\cdot}CuCr_2O_4$ (sol–gel)	hexyl acetate	0.55	45	74*
$Mn/Cu{\cdot}CuCr_2O_4$	hexyl acetate + pentyl acetate	0.24	61	90
$Mn/Cu{\cdot}CuCr_2O_4$ (sol–gel)	hexyl acetate + pentyl acetate	0.30	36	70*

Reaction conditions: $P_{H_2}=190$ atm, $T=220^{\circ}C$, catalyst/ester = 1/15 (w/w);

* equilibrium not reached

Table 2 lists results obtained for the hydrogenation of hexyl and pentyl acetate on both undoped and doped commercial and sol–gel catalysts, together with the corresponding width at half-height of the principal XRD line of Cu (30<2Θ<45) which is characteristic of the size of Cu metallic particles presumed to be the active phase of the catalyst. It can be seen that, after a reaction time of

2 or 4 h, the activity obtained with the sol–gel catalyst is fairly comparable with that of the corresponding industrial catalysts. This can be attributed to the reduction rate of the catalyst under the reaction conditions [8]:

$$CuO{\cdot}CuCr_2O_4 + H_2 \rightarrow Cu{\cdot}CuCr_2O_4 + H_2O$$

$$Cu{\cdot}CuCr_2O_4 + H_2 \rightarrow 2Cu/Cr_2O_3 + H_2O$$

For all catalysts, the reduction during the first cycle of the reaction produces water, which is assumed to act as a poison. Miya [8] and Laine [9] have reported that the removal of water increases the activity, avoiding sinterization phenomena. Figure 3c illustrates the rate of reduction (measured by TG–DTA) of some undoped and doped sol–gel and industrial copper chromite catalysts. It can be seen that the rates of reduction of the undoped and Mn-doped sol–gel catalysts are lower than those of the corresponding industrial ones. This behaviour can be attributed to a slower hydrogenation reaction of the esters with the sol–gel catalysts. For the Mn and Ba-doped sol–gel catalysts, the reaction is complete after ca 5.5 h, while for the undoped one more than 6 h is necessary.

Table 3 Hexyl acetate hydrogenation and metallic copper surface area for fresh Mn-doped copper chromite catalyst (industrial and sol–gel). First reaction cycle

Catalysts	#Metallic surface area of Cu after reaction/$m^2\ g^{-1}$	Hydrogenated hexyl acetate content/%		S_{BET}/ $m^2\ g^{-1}$ before reaction
		after 2 h	after 4 h	
$Mn/Cu{\cdot}CuCr_2O_4$ (Engelhard)	16	86	99	36
$Mn/Cu{\cdot}CuCr_2O_4$ (Sol–gel)	10	42	74*	94

Reaction conditions: P_{H_2}=190 atm, T=220°C, catalyst/ester = 1/15 (w/w)

* equilibrium not reached; # measured by N_2O adsorption [4]

Table 3 reports results for the hydrogenation of hexyl and pentyl acetate on both undoped and Mn-doped commercial and sol–gel catalysts, together with the corresponding metallic copper area measured by N_2O adsorption. The yield of the reaction again seems to be related to the metallic Cu surface, which is assumed to be the active phase of the catalyst. For the Mn-doped sol–gel catalyst, although the BET surface area is perceptibly higher than that of the corresponding industrial catalyst, its Cu metallic surface area is definitely lower relative to that for the commercial catalyst. For the sol–gel products, therefore, it can be concluded that the reduction of the catalyst leads to relevant sinterization phenomena which, by decreasing the metallic Cu surface area, lower the activity.

Conclusions

We have synthesized a copper chromite precursor via a new sol–gel methodology which allows the preparation of undoped or doped copper chromite catalyst. These catalysts have proved active in the hydrogenation of esters to the corresponding alcohols. A peculiarity of this preparation procedure is the possibility of obtaining the final catalyst after thermal activation at low temperature. The organic solvent used in the preparation step (propionic acid) can be recycled.

* * *

E. U. support (an individual Fellowship to A. K.) EBBR2 CT93-3053 is gratefully acknowledged.

References

1 H. Adkins, R. Conner and K. Folkers, J. Am. Chem. Soc., 53 (1931) 1091.
2 H. Boerma in 'Preparation of Catalyst', B. Delmon (Ed.), Elsevier Sci. Publ. Co., Amsterdam 1976, p. 105.
3 R. Prasad, Proceedings of the 10th International Congr. on Catalysis 'New Frontiers in Catalysis', Guczi et al. (ed.), 19–24 July, 1992, Budapest, Hungary.
4 J. W. Evans, M. S. Wainwright, A. J. Bridgewater and D. J. Young, Appl. Catal., 7 (1983) 75.
5 M. El Baydi, G. Poillerat, J. L. Rehspringer, J. L. Gautier, J. F. Koening and P. Chartier, J. of Solid Stat. Chem., 109 (1994) 281.
6 J. H. de Boer in 'Everett and F. Stone (eds), 'The Structure and Properties of Porous Materials', Butterworth, London 1958, p. 68.
7 E. Robens and G. Walter in F. Korte (eds), Methodicum Chimicum, Vol. 1, Part B, Academic Press, New York 1974, p. 678.
8 B. Miya, F. Hoshino and I. Wasa, J. Catal., 5 (1966) 401.
9 J. Laine and F. Severini, Appl. Catal., 65 (1990) 253.